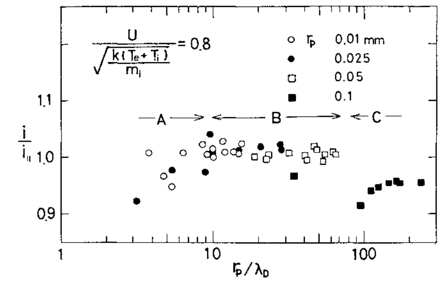

Fig. 2 Dependence of ion current on r_p/λ_D at $U/(k(T_e+T_i)/m_i)^{1/2}=0.8$.

$U/(kT_e/m_i)^{1/2}$ was used as the flow parameter. In this experiment, however, it is found that the probe response is influenced by the finite value of T_i/T_e as well as the flow speed. If the value of r_p/λ_D is same but T_i/T_e is not, the ion current variations cannot be interpreted by a single curve when $U/(kT_e m_i)^{1/2}$ is used as the parameter. If $U/(k(T_e+T_i)/m_i)^{1/2}$ is used instead of $U/(kT_e/m_i)^{1/2}$, the incoincidence disappears. Thus we take $U/(k(T_e+T_i)/m_i)^{1/2}$ as the flow parameter, although this theoretical interpretation is somewhat clouded.

The dependence of $i/i_{\parallel}$ on r_p/λ_D is shown in Figs. 2 and 3. In these figures, $U/(k(T_e+T_i)/m_i)^{1/2}$ is fixed at 0.8 and 1.5. It is found that the variation of $i/i_{\parallel}$ can be divided into three different regions of r_p/λ_D. It was seen also in Fig. 1. In the range C, the ion current falls off at first, has a minimum value and increases as the flow speed increases. For the value of r_p/λ_D under 10, the ion current monotonically decreases in this experiment. In the middle range B, the ion current increases monotonically. In the limit of $r_p/\lambda_D \to \infty$, we consider the ion current variations in a flowing plasma do not depend on r_p/λ_D significantly. Thus the two different responses of $i/i_{\parallel}$ in the range of $r_p/\lambda_D > 10$ should be caused by another factor. In the range C, λ_{ii}/r_p are smaller than unity, while λ_{in}/r_p ranges from 20–40 for 0.1 mm radius probe and 40–80 for 0.05 mm radius probe, respectively. Consequently, we consider that the ion-neutral collisions bring about the decrease of the ion current in the range C. Since the ion-neutral collisions can be ignored except for the large radius probes, the ion current responses in the range A and B are due to the interaction between the sheath surrounding the probe and the ion drift. The sheath in a flowing plasma may be thinner than one in a stationary plasma in front of, or on both sides of, the cylindrical probe and be blown away backward. This effect makes the probe current decrease. On the other hand, the ion drift motion makes it increase. For the probe with thick sheath, the decrease of the ion current due to the sheath deformation is larger than the increment due to the ion drift motion. Thus the total ion current decreases as the flow speed increases. For the probe with thin sheath, the increment of the ion current due to the ion drift is the predominant part of the ion current variation. Thus the total ion current increases for the thin sheath. As shown in Figs. 2 and 3, these reasons lead to the decrease of the ion current in the range of $r_p/\lambda_D < 10$, and the increment for the values of $r_p/\lambda_D > 10$.

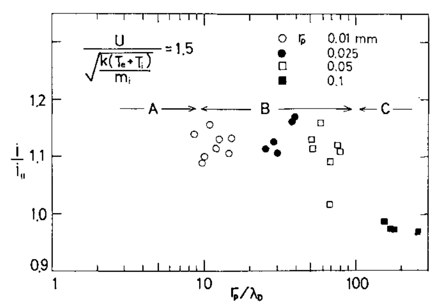

Fig. 3. Dependence of ion current on r_p/λ_D at $U/(k(T_e+T_i)/m_i)^{1/2}=1.5$.

In the range of A, λ_{in} is much larger than r_p and λ_{ii} is comparable with it. Thus the situation in which the ion current decreases in this experiment is quite different from that in the other experiments, in which it was described that the decreases of the ion current in the range of $r_p/\lambda_D \sim 1$ were due to the small values of λ_{ii}/r_p[7] or λ_{in}/r_p.[2] Stangeby and Allen[4] showed that the ion current decreased in the range of $r_p/\lambda_D \gg 1$ and $U/(kT_e/m_i)^{1/2} \ll 1$. This result disagrees with our experimental one. However, Swift-Hook and Andrews[5] showed that the ion current increased within the framework as Stangeby and Allen. This result showed the same trend as ours.

References

[1] Sonin, A. A., "Free-Molecule Langmuir Probe and Its Use in Flowfield Studies," *AIAA Journal*, Vol. 4, No. 9, Sept. 1966, pp. 1588–1596.

[2] Jakubowski, A. K., "Effect of Angle of Incidence on the Response of Cylindrical Electrostatic Probes at Supersonic Speeds," *AIAA Journal*, Vol. 10, No. 8, Aug. 1972, pp. 988–995.

[3] Laframboise, J. G., "Theory of Spherical and Cylindrical Langmuir Probes in a Collisionless, Maxwellian Plasma at Rest," UTILAS Rept. 100, 1966, University of Toronto, Toronto, Canada.

[4] Stangeby, P. C. and Allen, J. E., "Transonic Plasma Flow Past an Obstacle," *Journal of Plasma Physics*, Vol. 6, Pt. 1, 1971, pp. 19–32.

[5] Swift-Hook, D. T. and Andrews, J. G., "Cylindrical Probes in a Flowing Plasma," *Journal of Physics A: General Physics*, Vol. 4, No. 1, Jan. 1971, pp. L21–L24.

[6] Yoshikawa, T. and Murasaki, T., "Experimental Investigations on Arc-Heated Steady Plasma Flow," *Dynamics of Ionised Gases*; edited by M. I. Lighthill, I. Imai, and H. Sato, University of Tokyo Press, Tokyo, 1973, pp. 329–345.

[7] Hester, S. D. and Sonin, A A. "Ion Temperature Sensitive End Effect in Cylindrical Langmuir Probe Response at Ionosphere Satellite Conditions," *The Physics of Fluids*, Vol. 13, No. 5, May 1970, pp. 1265–1274.

Film Cooling by Oblique Slot Injection

R. H. Nilson* and Y. G. Tsuei†
University of Cincinnati, Cincinnati, Ohio

Introduction

WALL cooling by boundary-layer injection or transpiration is used in engineering applications.[1] The present investigation concerns the film cooling effectiveness of oblique injection from the wall into a compressible laminar boundary layer through single or multiple slots. Numerical solutions of the boundary-layer equations are obtained by a finite-difference method which has been extensively tested and found to be accurate, versatile, and very stable. Film cooling effectiveness is presented for a wide variety of injection configurations so that the effects of coolant mass flow, injection angle, boundary-layer thickness, slot width, and the presence of upstream cooling slots can be investigated. The results are interesting, and conclusions heretofore unreported are drawn regarding selection of film cooling parameters.

Received November 6, 1973; revision received December 26, 1973. This work was partially supported by U.S. Army Research Office—Durham, under Contract DAHC 04-69-C-0016.

Index category: Boundary Layers and Convective Heat Transfer—Laminar.

* Instructor and Graduate Student, Department of Mechanical Engineering.

† Associate Professor, Department of Mechanical Engineering. Member AIAA.

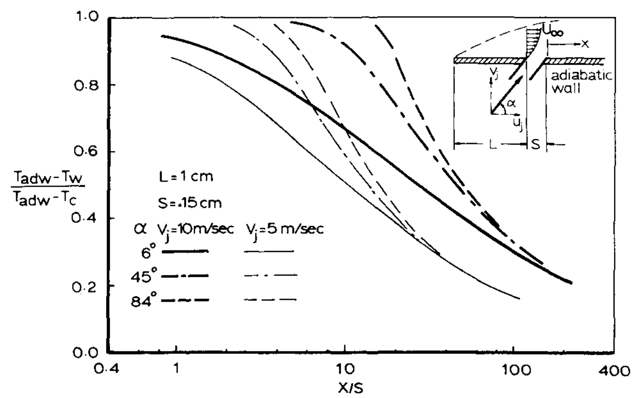

Fig. 1 Comparison of effectiveness for different coolant mass flow rates and injection angles.

Numerical Method

A finite-difference method is used to solve the following form of the boundary-layer equations:

$$\rho u \frac{\partial u}{\partial x} - \frac{\partial \psi}{\partial x}\frac{\partial u}{\partial y} = -\frac{dp}{dx} + \frac{\partial}{\partial y}\left(\mu \frac{\partial u}{\partial y}\right)$$

$$\rho u \frac{\partial T}{\partial x} - \frac{\partial \psi}{\partial x}\frac{\partial T}{\partial y} = \frac{u}{C_p}\frac{dp}{dx} + \frac{\partial}{\partial y}\left(\frac{\mu}{Pr}\frac{\partial T}{\partial y}\right) + \frac{\mu}{C_p}\left(\frac{\partial u}{\partial y}\right)^2$$

where the stream function ψ satisfies the requirements

$$\frac{\partial \psi}{\partial y} = \rho u \qquad \frac{\partial \psi}{\partial x} = -\left\{\rho_0 v_0 - \int_0^y \frac{\partial}{\partial x}(\rho u)\, dy\right\}$$

Although the present method traces its origin to that of Patankar and Spalding,[3] major modifications have been undertaken.[2] In deriving the difference equations, it is here assumed that u and T are piecewise linear in y, whereas in the Spalding method u and h° are taken to be piecewise linear in ψ. Since the latter assumption results in cuspid velocity and enthalpy profiles, it is believed that the present assumption is preferable. The method of grid expansion has been improved by the introduction of more extensive grid control devices and the Couette patching procedure of the Spalding method has been eliminated. The present method also includes programed checking of linearization assumptions with optional iteration or reduction in step size as required.

Test computations have been run for a variety of well documented flow configurations including wedge flows, flow over a cylinder, Howarth flow, compressible flows at various Mach numbers, incompressible flow at various Eckert numbers, wake flow, uniform suction and blowing, and slot suction. Excellent results were obtained as reported by Nilson and Tsuei.[2] Computation time on an IBM 370/165 is approximately 1500 forward steps, or roughly 10 runs/min.

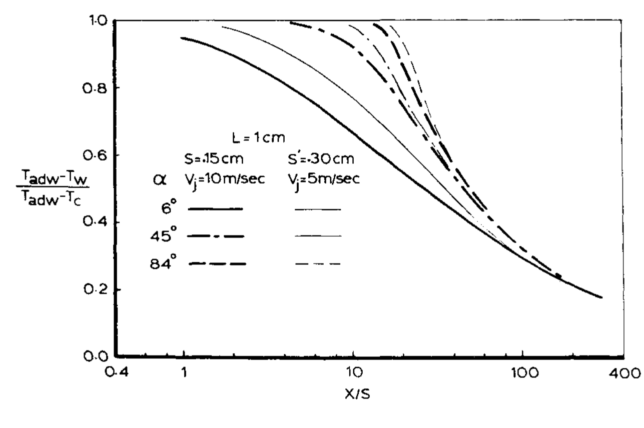

Fig. 2 Comparison of effectiveness for different slot widths.

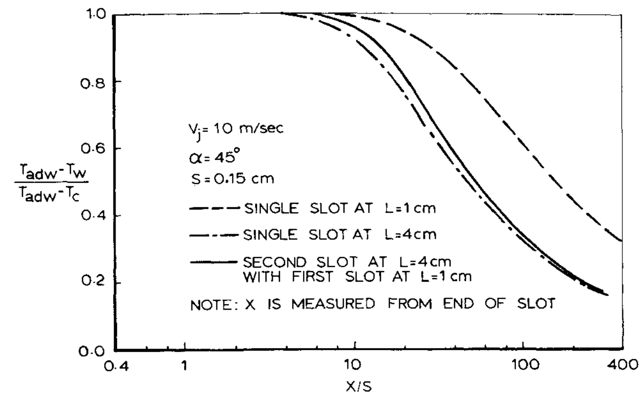

Fig. 3 Comparison of effectiveness for single slot and double slot injections.

Results

For the film cooling results reported here, the geometry is as shown in Fig. 1; the ambient velocity u_∞ is 50 m/sec, the ambient temperature T_∞ is 700°K, and the coolant temperature T_c is 350°K. Both the mainstream and the coolant are air at pressure, and in view of the large temperature difference, $T_\infty - T_c$, variations in density and viscosity are accounted for by the ideal gas law and Sutherland viscosity formula. Two different leading edge lengths, $L_1 = 1$ cm and $L_2 = 4$ cm, are included to show the effect of boundary-layer thickness on cooling effectiveness

$$\eta = (T_{adw} - T_w)/(T_{adw} - T_c)$$

(Note, in present case, the numerical value of adiabatic wall temperature T_{adw} is very close to that of the ambient temperature T_∞) and two different slot widths s, 0.15 cm and 0.30 cm, are used. The normal component v_j of injection velocity is chosen as 2, 5, and 10 m/sec to provide variation of the coolant mass flow $\dot{m}_c = \rho_c v_j s$. The ratios of the tangential velocity u_j to the normal velocity v_j at the injection slot are chosen as 10, 1, and 0.1. Thus, the oblique injection angles α measured from the main stream direction are approximately 6°, 45°, and 84° which, respectively, describe the features of the tangential, inclined, and normal injections. Double slot cooling is investigated with the first slot introduced at $L_1 = 1$ cm followed by a second slot at $L_2 = 4$ cm, both slots being of width $s = 0.15$ cm.

Figure 1 shows the influence of both the injection angle α and the coolant mass flow $\dot{m}_c$ on cooling effectiveness. Figure 2 presents the effect of varying s with $\dot{m}_c$ fixed, and Fig. 3 shows the effects of boundary-layer thickness and the presence of an upstream slot.

Discussion and Conclusions

An investigation of laminar film cooling by single or multiple slot injection is presented. Numerical solutions of the boundary-layer equations are obtained with a revised and improved version of the Patankar-Spalding method. Extensive testing has shown the present method to be versatile, accurate, and very stable. From the results presented here, several qualitative conclusions are drawn regarding the selection of film cooling parameters such as slot length s, slot location L, injection angle α, and coolant mass flow $\dot{m}_c$.

1) As indicated in Fig. 1, normal injection provides greater effectiveness than tangential injection in the region immediately downstream of the slot because of the greater thickening effect on the boundary layer which reduces heat transfer. Thus, if high effectiveness, say 0.5, must be maintained, normal injection is preferred and will allow wider spacing of cooling slots. However, it is noted that for a given coolant flow rate, normal injection causes much greater boundary-layer growth than tangential injection and thus may induce early separation which decreases aerodynamic performance. A qualitatively similar heat-

transfer phenomenon is reported by Sherman et al.[4] in a numerical study of laminar parallel slot injection wherein it is found that, for the same coolant flow, increasing slot height provides more effective cooling than increasing jet velocity. As expected, the boundary-layer thickening and insulating effect observed in parallel slot injection is more pronounced than that reported here for oblique injection. However, the parallel slot configuration is not suitable for engineering applications such as turbine blade cooling.

2) As indicated in Fig. 1, well downstream of the slot, the cooling effectiveness of tangential injection is nearly equal to that of normal injection. Thus, if only moderate effectiveness, say 0.3, is required, it is preferable to use tangential injection, which not only serves the purpose of film cooling but also increases aerodynamic performance. In general, a compromise must be considered in film cooling design.

3) As indicated in Fig. 2, where coolant mass flow is held fixed, a low injection velocity with a wide slot is preferable to a high velocity with a narrow slot. Although the effect is small for normal injection, it is more pronounced for tangential injection.

4) As indicated in Fig. 3, the larger the boundary-layer thickness upstream of the slot, the greater the effectiveness, particularly near the slot region. However, this influence diminishes as the injection angle α is decreased.

5) As indicated in Fig. 3, the presence of an upstream slot increases cooling effectiveness. However, the degree of influence is strongly dependent on the spacing between slots, since the increased efficiency is primarily attributed to the reduction of temperature in the boundary layer, with increase of boundary-layer thickness being a secondary consideration.

References

[1] Goldstein, R. J., "Film Cooling," *Advances in Heat Transfer*, Vol. 7, 1971, pp. 321–379.

[2] Nilson, R. H. and Tsuei, Y. G., "A Numerical Method for Boundary Layer Equations," Report, Jan. 1974, Dept. of Mechanical Engineering, Univ. of Cincinnati, Cincinnati, Ohio.

[3] Patankar, S. V. and Spalding, D. B., "A Finite Difference Procedure for Solution of the Equations of the Two Dimensional Boundary Layer," *International Journal of Heat and Mass Transfer*, Vol. 10, No. 10, 1967, pp. 1389–1412.

[4] Sherman, A., Yeh, H., McAssey, E., and Reshotko, E., "Multiple Slot Laminar Film Cooling," *AIAA Journal*, Vol. 11, No. 10, Oct. 1973, pp. 1413–1414.

Combined Effects of Nose Bluntness and Cone Angle on Unsteady Aerodynamics

L. E. Ericsson,* R. A. Guenther,† W. R. Stake,† and G. S. Olmsted†

Lockheed Missiles and Space Company, Inc., Sunnyvale, Calif.

NOSE bluntness effects play an important role in aerodynamics of slender bodies in hypersonic flow. When trying to use experimental data for blunted slender cones one encounters the problem that more than one of the geometric parameters, e.g., cone frustum angle and nose bluntness, have been changed between tests. Cone angles of 5°–20° have been used in combinations with nose bluntnesses from zero to $(d_N/d_B) = 0.50$. If through the selection of suitable scaling para-

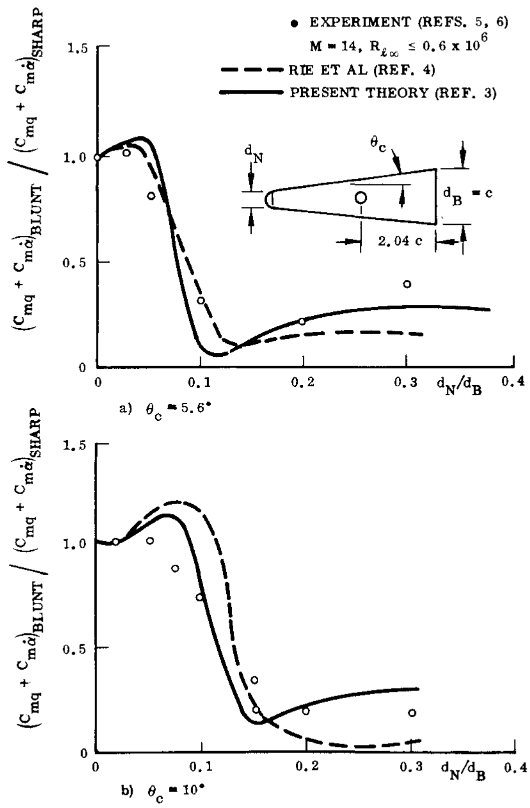

Fig. 1 Comparison between predicted and measured effect of nose bluntness on slender cone damping at $\alpha = 0$.

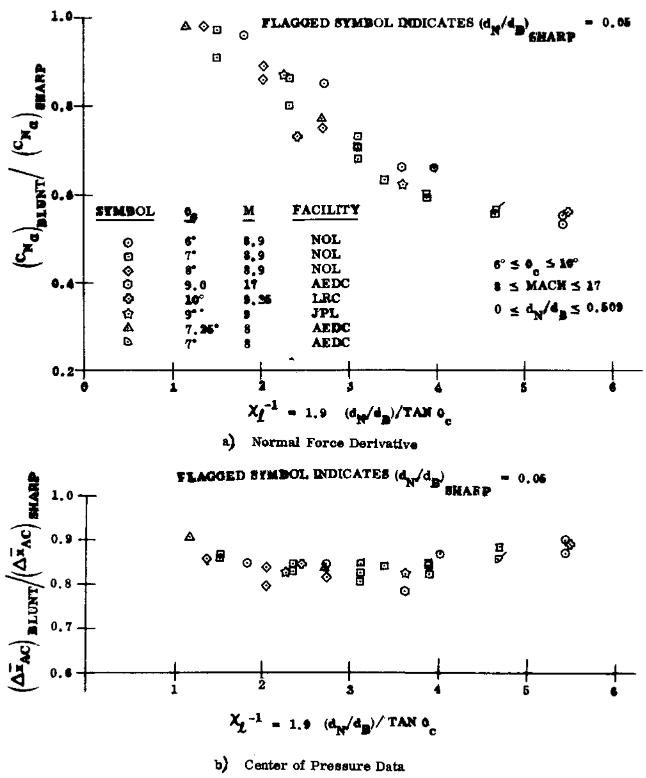

Fig. 2 Scaling of experimental static data for slender blunted cones.

Received November 12, 1973; revision received January 10, 1974.

Index categories: Entry Vehicle Dynamics and Control; Nonsteady Aerodynamics; Supersonic and Hypersonic Flow.

* Consulting Engineer. Associate Fellow AIAA.

† Aerodynamics Engineer, Senior.